Article

Mechanical Bond-Protected Air-Stable Radicals

Junling Sun, Zhichang Liu, Wei-Guang Liu, Yilei Wu, Yuping Wang, Jonathan C. Barnes, Keith R. Hermann, William A. Goddard, Michael R. Wasielewski, and J. Fraser Stoddart

J. Am. Chem. Soc., **Just Accepted Manuscript** • DOI: 10.1021/jacs.7b06857 • Publication Date (Web): 14 Aug 2017

JOURNAL OF THE AMERICAN CHEMICAL SOCIETY

Mechanical Bond-Protected Air-Stable Radicals

Junling Sun,[#,1] Zhichang Liu,*[,#,1] Wei-Guang Liu,[3] Yilei Wu,[1] Yuping Wang,[1]

Jonathan C. Barnes,[1,4] Keith R. Hermann,[1] William A. Goddard III,[3] Michael R. Wasielewski,[1,2]

and J. Fraser Stoddart[1,*]

[1]*Department of Chemistry and* [2]*Argonne-Northwestern Solar Energy Research (ANSER) Center, Northwestern University, 2145 Sheridan Road, Evanston, IL 60208, USA*

[3]*Materials and Process Simulation Center, California Institute of Technology, Pasadena, CA 91125, USA*

[4]*Department of Chemistry, Washington University, One Brookings Drive, St. Louis, MO 91125, USA*

*E-mail: zhichang-liu@northwestern.edu, stoddart@northwestern.edu

MAIN TEXT

ABSTRACT: Radical templation centered around a heterotrisradical tricationic inclusion complex $\mathbf{DB}^{\bullet+}\subset\mathbf{DAPQT}^{2(\bullet+)}$, assembled from an equimolar mixture of a disubstituted 4,4'-bipyridinium radical cation ($\mathbf{DB}^{\bullet+}$) and an asymmetric cyclophane bisradical dication ($\mathbf{DAPQT}^{2(\bullet+)}$), affords a symmetric [2]catenane ($\mathbf{SC}\bullet 7PF_6$) and an asymmetric [2]catenane ($\mathbf{AC}\bullet 7PF_6$) on reaction of the 1:1 complex with diazapyrene and bipyridine, respectively. Both these highly charged [2]catenanes have been isolated as air-stable mono-radicals and characterized by EPR spectroscopy. X-Ray crystallography reveals that the unpaired electrons are delocalized in each case across two inner 4,4'-bipyridinium ($BIPY^{2+}$) units forming a mixed-valence $(BIPY_2)^{\bullet 3+}$ state inside both [2]catenanes, an observation which is in good agreement with spin-density calculations using density functional theory. Electrochemical studies indicate that by replacing the $BIPY^{2+}$ units in homo[2]catenane $\mathbf{HC}^{\bullet 7+}$—composed of two mechanically interlocked cyclobis(paraquat-*p*-phenylene) rings—with 0, 1, and 2 more highly conjugated diazapyrenium dication (DAP^{2+}) units, respectively, a consecutive series of 5, 6, and 7 redox states can be accessed in the resulting $\mathbf{SC}\bullet 7PF_6$ (0, 4+, 6+, 7+, and 8+), $\mathbf{HC}\bullet 7PF_6$ (0, 2+, 4+, 6+, 7+, and 8+), and $\mathbf{AC}\bullet 7PF_6$ (0, 1+, 2+, 4+, 6+, 7+, and 8+), respectively. These unique [2]catenanes present a promising prototype for the fabrication of high-density data memories.

■ INTRODUCTION

Ever since the landmark discovery of the triphenylmethyl radical[1] by Moses Gomberg, research on stable organic radicals[2] has attracted attention, not only on account of their exotic electronic properties, but also because of their potential applications as spin-labels[3] and in organic lithium batteries[4] as well as in conductive and magnetic materials.[5] To date, however, most organic radicals experience a fleeting existence and readily undergo dimerization and/or

oxidation. The synthesis and isolation of persistent radicals in crystalline forms remains a challenge. In addition, molecular systems with adjustable number of accessible redox states are quite difficult to achieve.

4,4'-Bipyridinium radical cations ($BIPY^{\bullet+}$) tend to form[6] $(BIPY^{\bullet+})_2$ dimers in a 'face-to-face' manner in the solid state as a result of favorable radical-pairing interactions. Conversely, in a dilute solution, $(BIPY^{\bullet+})_2$ dimers are prone[7] to dissociate because of their low association constants. Recently, however, we found[8] that a cyclobis(paraquat-*p*-phenylene) bisradical dication ($\mathbf{CBPQT}^{2(\bullet+)}$) and a $BIPY^{\bullet+}$ radical cation are capable of assembling to afford a stable trisradical tricationic inclusion complex $BIPY^{\bullet+}\subset\mathbf{CBPQT}^{2(\bullet+)}$ in MeCN, assisted by radical-pairing interactions. This 1:1 inclusion complex has been investigated extensively and employed in recognition motifs, either to template[9] the formation of, otherwise difficult to synthesize highly energetic mechanically interlocked molecules (MIMs), or to enhance[10] the switching performance of bistable MIMs. In particular, we have been able to synthesize[9] (Figure 1) an air- and water-stable paramagnetic homo[2]catenane $\mathbf{HC}^{\bullet7+}$ from the trisradical complex $\mathbf{DB}^{\bullet+}\subset\mathbf{CBPQT}^{2(\bullet+)}$. Up to six redox states of this [2]catenane can be accessed electrochemically.

Herein we demonstrate a molecular system—namely, a novel class of octacationic [2]catenanes—which exhibits adjustable multiple accessible redox states. We report the radical template-directed syntheses of two analogues (Figure 1) of $\mathbf{HC}^{\bullet7+}$—namely, the asymmetric [2]catenane $\mathbf{AC}^{\bullet7+}$ and the symmetric [2]catenane $\mathbf{SC}^{\bullet7+}$—by incorporating simultaneously both the less conjugated $BIPY^{2+}$ and the more highly conjugated 2,7-diazapyrenium (DAP^{2+}) units into the [2]catenane structures in order to modulate the number of the accessible redox states of the resulting molecules. We show that these [2]catenanes, which exist as persistent air-stable radicals, can exist in a consecutive series of 5 ($\mathbf{SC}^{\bullet7+}$: 0, 4+, 6+, 7+, and 8+), 6 ($\mathbf{HC}^{\bullet7+}$: 0, 2+, 4+,

6+, 7+, and 8+), and 7 ($\mathbf{AC}^{\bullet 7+}$: 0, 1+, 2+, 4+, 6+, 7+, and 8+) redox states. We have characterized these mixed-valence and other redox states by (i) electron paramagnetic resonance (EPR) and UV-Vis-NIR spectroscopies, (ii) high-resolution mass spectrometry (HR-MS), (iii) single crystal X-ray diffraction (XRD) analysis, and (iv) electrochemical means as well as (v) density functional theory (DFT) calculations.

■ RESULTS AND DISCUSSION

Since the N–N distances in both DAP^{2+} and $BIPY^{2+}$ dications are[11] essentially identical, and DAP^{2+} dications are known to undergo[12] the one-electron reduction to form the corresponding $DAP^{\bullet+}$ radical cations, DAP^{2+} dications were selected as substitutes for the $BIPY^{2+}$ units in $\mathbf{HC}^{\bullet 7+}$. The redox properties of the *N*,*N*'-dimethyl-2,7-diazapyrenium dication ($\mathbf{MDAP}^{2+}$) were explored by variable scan-rate cyclic voltammetry (CV) and compared with those of 1,1'-dimethyl-4,4'-bipyridinium ($\mathbf{MV}^{2+}$). CV of $\mathbf{MDAP}^{2+}$ at 10 mV s^{-1} reveals (Figure 2a, black trace) that the reduction of $\mathbf{MDAP}^{2+}$ to $\mathbf{MDAP}^{\bullet+}$ occurs at a potential of –450 mV, which is similar to that of –480 mV for $\mathbf{MV}^{2+}$. As the scan rate is increased, the reduction wave remains the same, but the intensity of the original oxidation wave at –370 mV gradually decreases, and meanwhile a new oxidation wave appears at +40 mV. Eventually, at the scan rate of 1 V s^{-1} (Figure 2a, purple trace), two oxidation waves reach the same intensity. These observations indicate[13] that, in solution, the $\mathbf{MDAP}^{\bullet+}$ radical cations exist primarily as cationic radical dimers $(\mathbf{MDAP}^{\bullet+})_2$, wherein oxidation leads firstly to the formation of a single unpaired spin mixed-valence dimer $(\mathbf{MDAP}_2)^{\bullet 3+}$ before it completely dissociates into two $\mathbf{MDAP}^{2+}$ dications. When the scan rate is slower than the time scale of the dissociation of $(\mathbf{MDAP}_2)^{\bullet 3+}$, oxidation of $(\mathbf{MDAP}^{\bullet+})_2$ is observed to occur as a single oxidation wave. Once the scan rate becomes faster than the dissociation rate, however, two separate oxidation waves corresponding to

$(\mathbf{MDAP}^{\bullet+})_2 \rightarrow (\mathbf{MDAP}_2)^{\bullet 3+}$ and $(\mathbf{MDAP}_2)^{\bullet 3+} \rightarrow 2\ \mathbf{MDAP}^{2+}$ can be observed. In contrast to $\mathbf{MDAP}^{\bullet+}$, the $\mathbf{MV}^{\bullet+}$ radical cations exist mainly as monomers. It can be concluded that, in addition to radical pairing interactions, the $(\mathbf{MDAP}^{\bullet+})_2$ dimers are most likely further stabilized[14] by additional [π···π] interactions between the large aromatic π-surfaces of $\mathbf{MDAP}^{\bullet+}$.

In the knowledge that both $\mathbf{MDAP}^{2+}$ and $\mathbf{MV}^{2+}$ can be reduced to their corresponding radical cationic states at similar potentials, we explored the possibility of forming trisradical tricationic complexes between $DAP^{\bullet+}$ and $BIPY^{\bullet+}$ units. Upon reducing[15] an equimolar mixture of a 1,1'-disubstituted 4,4'-bipyridinium salt ($\mathbf{DB}\bullet 2PF_6$) and $\mathbf{DAPQT}\bullet 4PF_6$ in MeCN, a purple solution was obtained. Its UV-Vis-NIR spectrum exhibits (Figure 2b) an absorption band centered on 920 nm, which is characteristic of radical cationic $(BIPY^{\bullet+})_2$ dimers.[16] This observation implies that the $DAP^{\bullet+}$ unit in $\mathbf{DAPQT}^{2(\bullet+)}$ interacts with the $\mathbf{DB}^{\bullet+}$ radical cation very weakly if at all and the radical-pairing interaction is mainly associated with the interaction between the two $BIPY^{\bullet+}$ units and the $\mathbf{DB}^{\bullet+}$ radical cation. The association constant (K_a) of $\mathbf{DB}^{\bullet+} \subset \mathbf{DAPQT}^{2(\bullet+)}$ was determined (Figure S7) to be $(8.9 \pm 5.5) \times 10^3\ M^{-1}$ in MeCN by UV-Vis-NIR titration. It is[8] smaller than the one ($K_a = 5.0 \times 10^4\ M^{-1}$) observed for $\mathbf{DB}^{\bullet+} \subset \mathbf{CBPQT}^{2(\bullet+)}$, suggesting that the $DAP^{\bullet+}$ unit does not interact strongly with $\mathbf{DB}^{\bullet+}$. An attempt to form the hetero trisradical tricationic complex $\mathbf{MDAP}^{\bullet+} \subset \mathbf{CBPQT}^{2(\bullet+)}$ was not successful as indicated (Figure S6) by the absence of a NIR absorption band in its UV-Vis-NIR spectrum. This failure to form a 1:1 inclusion complex reflects the fact that the cavity of $\mathbf{CBPQT}^{2(\bullet+)}$ is not large enough to accommodate $\mathbf{MDAP}^{\bullet+}$.

Single crystals of a 1:1 inclusion complex which does form were obtained by slow vapor diffusion of $^{i}Pr_2O$ into an MeCN solution of an equimolar mixture of $\mathbf{DB}^{\bullet+}$ and $\mathbf{DAPQT}^{2(\bullet+)}$ in an Ar-filled glovebox. The solid-state superstructure (Figures 2c and S9) reveals that each inclusion complex is surrounded by four PF_6^- counterions, an observation which indicates[17] that the

complex is indeed the bisradical tetracation ((**DB**⊂**DAPQT**)$^{2\bullet 4+}$) rather than a trisradical trication in the solid state. Since the torsional angles of both units **A** and **B** are less than 3° and the plane-to-plane separation between them is only 3.1 Å, the implication is that both units **A** and **B** are in the radical cationic BIPY$^{\bullet+}$ state and the remaining unit **C** is in the dicationic DAP^{2+} state. The plane-to-plane separation between units **B** and **C** is 3.4 Å, a distance which is a typical one for [π···π] interactions. In addition, the complex is further stabilized by multiple [C–H···π] interactions between the *p*-phenylene rings on the unit **B** and C–H groups on the DAP^{2+} unit. Overall, the superstructure is arranged (Figure 2d) in an infinite stack, driven by intermolecular [Br···π] interactions between adjacent inclusion complexes.

Since the hetero trisradical tricationic complex is stable in MeCN, we grasped[18] the opportunity to synthesize (Schemes S1 and S2) **AC**•7PF_6 and **SC**•7PF_6. The *in situ* formed complex **DB**$^{\bullet+}$⊂**DAPQT**$^{2(\bullet+)}$ was allowed to react with 4,4'-bipyridine and 2,7-diazapyrene, respectively, for two weeks at room temperature to afford both **AC**•7PF_6 and **SC**•7PF_6 as purple solids. The ^{1}H NMR spectra of both catenanes were obtained for their fully oxidized states **AC**•8PF_6 and **SC**•8PF_6 which were prepared by oxidizing the as-synthesized catenanes with an excess of NO•PF_6. **AC**$^{8+}$ possesses a time-averaged C_{2v} symmetry and hence displays (Figure 3b) a relatively complicated ^{1}H NMR spectrum on account of the interlock-induced desymmetrization. It is worth highlighting that the proton resonances for $H_{\beta 2}$ and $H_{\beta 3}$, belonging to the two innermost BIPY^{2+} units are shifted dramatically upfield by 3.9 and 4.6 ppm because of the strong shielding effect imposed by their accompanying cyclophanes. The slightly larger upfield shift observed for $H_{\beta 3}$ is ascribed to the stronger shielding effect on $H_{\beta 3}$ exerted by the DAP^{2+} unit on **DAPQT**$^{4+}$. **SC**$^{8+}$, which has a higher time-averaged D_{2d} symmetry, exhibits

(Figure S3) a comparatively simple ^{1}H NMR spectrum and is also characterized by the upfield shifted H_β.

In order to confirm beyond any doubt that the as-synthesized catenanes exist as persistent stable radicals, we performed EPR measurements. The results reveal (Figure 4a) that both catenanes are EPR active, an observation which is in good agreement with their containing an unpaired electron. Moreover, the spectra display indiscernible hyperfine splitting, an observation which suggests that rapid spin exchange exists within both catenanes. This conclusion is also supported[19] (Figure 4b) by the NIR absorption bands centered on ca. 1415 nm in their UV-Vis-NIR spectra.

In order to gain more insight into the location of the delocalized radical electron, single crystal XRD analyses were performed on single crystals of **AC**•7PF_6 and **SC**•7PF_6. The solid-state structures demonstrate (Figures 4c and d, S10 and S11) that each catenane crystallizes with 7 PF_6^- counterions, an observation which is consistent with their mono-radical states. In the case of **AC**$^{\bullet 7+}$, the torsional angle of 34° for the unit **D**, is typical for the dicationic $BIPY^{2+}$ unit and tells us that the unpaired electron is not located on the unit **D**. By contrast, units **B** and **C** have smaller torsional angles—namely, 8° and 10°, respectively—and thus the heterocyclic rings can be deemed as being almost coplanar. The flattening effect suggests that the unpaired electron is shared by units **B** and **C**. This conclusion is further supported by their short plane-to-plane separation, which is only 3.1 Å being[9] typical for single unpaired spin interactions. The large plane-to-plane separation (3.5 Å) between units **A** and **B** suggests that the unit **A** is unlikely to be involved in the electron sharing. In the same manner, it can be argued that the unpaired electron in **SC**$^{\bullet 7+}$ is shared by units **B** (8°) and **C** (10°) as well. Along with the observations for **HC**$^{\bullet 7+}$, it

can be concluded that the change from $BIPY^{2+}$ to DAP^{2+} does not affect the location of the unpaired electrons.

DFT Calculations were performed on $\mathbf{AC}^{\bullet 7+}$ and $\mathbf{SC}^{\bullet 7+}$ in order to probe their electronic properties. The results illustrate (Figure S12) that the spin densities in both catenanes are located on their two inner $BIPY^{2+/\bullet+}$ units in line with the experimental results. The efficient electron delocalization across the two inner $BIPY^{2+/\bullet+}$ units could be one of the primary reasons for the stabilization of these radicals. The theoretical binding energies (Table S1) for the formation of catenanes from the corresponding cyclophanes were calculated[20] in MeCN at the M06/6-311++G** level. For both catenanes, the formation of the 8+ state has a significant larger unfavorable energy than that of the corresponding 7+ state and provides an explanation for the high resistance of the 7+ state towards oxidation.

The redox properties of $\mathbf{AC}^{\bullet 7+}$ and $\mathbf{SC}^{\bullet 7+}$ were investigated employing electrochemistry and compared with that of $\mathbf{HC}^{\bullet 7+}$. Differential pulse voltammetry (DPV) reveals that $\mathbf{AC}^{\bullet 7+}$ exhibits (Figure 5c) up to six redox processes and as many as seven discrete accessible redox states on account of its low symmetry, whereas $\mathbf{SC}^{\bullet 7+}$ has (Figure 5a) only four redox processes and five redox states. In contrast, there are five redox processes and six redox states in the differential pulse voltammogram (Figure 5b) of $\mathbf{HC}\bullet 7PF_6$. These observations indicate the fact that the introduction of the DAP^{2+} units to replace the $BIPY^{2+}$ units can precisely modulate the stereoelectronic effect in this octacationic [2]catenane system. As a consequence, a consecutive series of five, six, and seven redox states are achieved in the resulting $\mathbf{SC}\bullet 7PF_6$ (0, 4+, 6+, 7+, and 8+), $\mathbf{HC}\bullet 7PF_6$ (0, 2+, 4+, 6+, 7+, and 8+), and $\mathbf{AC}\bullet 7PF_6$ (0, 1+, 2+, 4+, 6+, 7+, and 8+), respectively, which render these catenanes ideal for applications as memory devices. In particular, all these redox states can be accessed at low potentials, ranging from –1.1 to +0.5 V,

which guarantee very low write and erase voltages. As such, these three catenanes hold considerable promise in relation to creating high-density memory devices with low energy consumption.[21]

■ CONCLUSIONS

In summary, we have demonstrated that the **DB**$^{\bullet+}$ radical cation and the asymmetric cyclophane bisradical dication **DAPQT**$^{2(\bullet+)}$ enable the formation of a stable heterotrisradical tricationic inclusion complex **DB**$^{\bullet+}$⊂**DAPQT**$^{2(\bullet+)}$ with an association constant of $(8.9 \pm 5.5) \times 10^3$ M^{-1} in MeCN. This complex is stabilized by (i) radical-pairing reactions between **DB**$^{\bullet+}$ and the BIPY$^{\bullet+}$ unit of **DAPQT**$^{2(\bullet+)}$, (ii) [π···π] stacking between **DB**$^{\bullet+}$ and the DAP$^{\bullet+}$ unit of **DAPQT**$^{2(\bullet+)}$, and (iii) [C–H···π] interactions. Taking advantage of the radical templation of **DB**$^{\bullet+}$⊂**DAPQT**$^{2(\bullet+)}$, we have prepared two catenanes, **AC**$^{\bullet7+}$ and **SC**$^{\bullet7+}$, both of which are air-stable persistent radicals. In particular, electrochemical studies indicate that, by replacing the BIPY^{2+} units with zero, one, and two the more conjugated DAP^{2+} units, a consecutive series of five, six, and seven redox states can be accessed electrochemically in the resulting **SC**•7PF_6 (0, 4+, 6+, 7+, and 8+), **HC**$^{\bullet7+}$ (0, 2+, 4+, 6+, 7+, and 8+), and **AC**•7PF_6 (0, 1+, 2+, 4+, 6+, 7+, and 8+), respectively, rendering this unique series of catenanes promising prototypes in the development of high-density data memories.

■ ASSOCIATED CONTENT

Supporting Information

Detailed information regarding the experimental methods and procedures, X-ray crystallographic data, and supportive figures and tables. This material is available free of charge via the Internet at http://pubs.acs.org. CIF files for (**DB**⊂**DAPQT**)•4PF_6, **AC**•7PF_6 and **SC**•7PF_6 (CCDC 1559720–1559722).

AUTHOR INFORMATION

Corresponding Authors

zhichang-liu@northwestern.edu
stoddart@northwestern.edu

Author Contributions

[#]J. Sun and Z. Liu contributed equally.

Notes

The authors declare no competing financial interest.

ACKNOWLEDGEMENTS

This research is part of the Joint Center of Excellence in Integrated Nano-Systems (JCIN) at King Abdulaziz City for Science and Technology (KACST) and Northwestern University (NU). The authors thank both KACST and NU for their continued support of this research. The computational studies at Caltech were supported by NSF EFRI-1332411 (ODISSEI). This work was also supported by National Science Foundation grant no. CHE-1565925 (M.R.W.)

REFERENCES

(1) Gomberg, M. *J. Am. Chem. Soc.* **1900**, *22*, 757.

(2) (a) Nishinaga, T.; Komatsu, K. *Org. Biomol. Chem.* **2005**, *3*, 561; (b) Zaitsev, V.; Rosokha, S. V.; Head-Gordon, M.; Kochi, J. K. *J. Org. Chem.* **2006**, *71*, 520; (c) *Stable Radicals: Fundamentals and Applied Aspects of Odd-Electron Compounds*; Hicks, R., Ed.; Wiley, New York 2011; (d) Wen, J.; Havlas, Z.; Michl, J. *J. Am. Chem. Soc.* **2015**, *137*, 165.

(3) Cafiso, D. S. *Acc. Chem. Res.* **2014**, *47*, 3102.

(4) (a) Morita, Y.; Nishida, S.; Murata, T.; Moriguchi, M.; Ueda, A.; Satoh, M.; Arifuku, K.; Sato, K.; Takui, T. *Nat. Mater.* **2011**, *10*, 947; (b) Aqil, A.; Vlad, A.; Piedboeuf, M.-L.; Aqil, M.; Job, N.; Melinte, S.; Detrembleur, C.; Jerome, C. *Chem. Commun.* **2015**, *51*, 9301.

(5) (a) Hünig, S.; Erk, P. *Adv. Mater.* **1991**, *3*, 225; (b) Hicks, R. G.; Lemaire, M. T.;

Öhrström, L.; Richardson, J. F.; Thompson, L. K.; Xu, Z. *J. Am. Chem. Soc.* **2001**, *123*, 7154; (c) Tasoglu, S.; Yu, C. H.; Gungordu, H. I.; Guven, S.; Vural, T.; Demirci, U. *Nat. Commun.* **2014**, *5*, 4702; (d) Oliva, J.; Alcoba, D.; Oña, O.; Torre, A.; Lain, L.; Michl, J. *Theor. Chem. Acc.* **2015**, *134*, 1.

(6) Kosower, E. M.; Cotter, J. L. *J. Am. Chem. Soc.* **1964**, *86*, 5524.

(7) In solution, the $(BIPY^{\bullet+})_2$ radical cationic dimers can be stabilized in the presence of receptors. See example: Jeon, W. S.; Ziganshina, A. Y.; Lee, J. W.; Ko, Y. H.; Kang, J.-K.; Lee, C.; Kim, K. *Angew. Chem. Int. Ed.* **2003**, *42*, 4097.

(8) Fahrenbach, A. C.; Barnes, J. C.; Lanfranchi, D. A.; Li, H.; Coskun, A.; Gassensmith, J. J.; Liu, Z.; Benítez, D.; Trabolsi, A.; Goddard, W. A., III; Elhabiri, M.; Stoddart, J. F. *J. Am. Chem. Soc.* **2012**, *134*, 3061.

(9) Barnes, J. C.; Fahrenbach, A. C.; Cao, D.; Dyar, S. M.; Frasconi, M.; Giesener, M. A.; Benítez, D.; Tkatchouk, E.; Chernyashevskyy, O.; Shin, W. H.; Li, H.; Sampath, S.; Stern, C. L.; Sarjeant, A. A.; Hartlieb, K. J.; Liu, Z.; Carmieli, R.; Botros, Y. Y.; Choi, J. W.; Slawin, A. M. Z.; Ketterson, J. B.; Wasielewski, M. R.; Goddard, W. A., III; Stoddart, J. F. *Science* **2013**, *339*, 429.

(10) (a) Zhu, Z.; Fahrenbach, A. C.; Li, H.; Barnes, J. C.; Liu, Z.; Dyar, S. M.; Zhang, H.; Lei, J.; Carmieli, R.; Sarjeant, A. A.; Stern, C. L.; Wasielewski, M. R.; Stoddart, J. F. *J. Am. Chem. Soc.* **2012**, *134*, 11709. (b) Sun, J.; Wu, Y.; Wang, Y.; Liu, Z.; Cheng, C.; Hartlieb, K. J.; Wasielewski, M. R.; Stoddart, J. F. *J. Am. Chem. Soc.* **2015**, *137*, 13484.

(11) Ashton, P. R.; Boyd, S. E.; Brindle, A.; Langford, S. J.; Menzer, S.; Pérez-Garcia, L.; Preece, J. A.; Raymo, F. M.; Spencer, N.; Stoddart, J. F.; White, A. J. P.; Williams, D. J. *New J. Chem.* **1999**, *23*, 587.

(12) Lilienthal, N. D.; Enlow, M. A.; Othman, L.; Smith, E. A. F.; Smith, D. K. *J. Electroanal. Chem.* **1996**, *414*, 107.

(13) It is also possible that the $\mathbf{MDAP}^{\bullet+}$ radical cation forms oliogomers in addition to dimer.

(14) DAP^{2+} dications are known to be good π-acceptors. See example: Rama, T.; López-Vidal, E. M.; García, M. D.; Peinador, C.; Quintela, J. M. *Chem. Eur. J.* **2015**, *21*, 9482.

(15) The reduction was carried out by the addition of an excess of Zn dust to the mixture of **DB**•$2PF_6$ and **DAPQT**•$4PF_6$ in MeCN. After stirring the suspension for 30 min, the unreacted Zn dust was filtered off.

(16) Chen, L.; Wang, H.; Zhang, D. W.; Zhou, Y.; Li, Z. T. *Angew. Chem. Int. Ed.* **2015**, *54*, 4028.

(17) The bisradical tetracationic state could be the result of partial oxidation during crystallization, especially since the $DAP^{\bullet+}$ radical cation does not interact efficiently with $\mathbf{DB}^{\bullet+}$. Such a situation has also been observed in several other systems. See example: Cheng, C.; McGonigal, P. R.; Liu, W.-G.; Li, H.; Vermeulen, N. A.; Ke, C.; Frasconi, M.; Stern, C. L.; Goddard, W. A., III; Stoddart, J. F. *J. Am. Chem. Soc.* **2014**, *136*, 14702.

(18) See SI for the details.

(19) Barnes, J. C.; Frasconi, M.; Young, R. M.; Khdary, N. H.; Liu, W.-G.; Dyar, S. M.; McGonigal, P. R.; Gibbs-Hall, I. C.; Diercks, C. S.; Sarjeant, A. A.; Stern, C. L.; Goddard, W. A., III; Wasielewski, M. R.; Stoddart, J. F. *J. Am. Chem. Soc.* **2014**, *136*, 10569.

(20) Zhao, Y.; Truhlar, D. *Theor. Chem. Acc.* **2008**, *120*, 215.

(21) Recently, considerable efforts have been devoted to developing multilevel memories in order to increase data density. One effective way is ((a) Busche, C.; Vila-Nadal, L.; Yan, J.; Miras, H. N.; Long, D.-L.; Georgiev, V. P.; Asenov, A.; Pedersen, R. H.; Gadegaard, N.; Mirza, M. M.; Paul, D. J.; Poblet, J. M.; Cronin, L. *Nature* **2014**, *515*, 545. (b) Liu, Z.; Shi, E.; Wan, Y.; Li, N.; Chen, D.; Xu, Q.; Li, H.; Lu, J.; Zhang, K.; Wang, L. *J. Mater. Chem. C* **2015**, *3*, 2033.) to utilize a collection of redox-active molecules wherein information can be stored in discrete redox states. As a result, increasing the number of redox states within a single molecule can potentially help to realize the high density data storage.

Captions to Figures

Figure 1. Structural formulas of the three radical catenanes **HC**•7PF_6, **SC**•7PF_6 and **AC**•7PF_6 (top), and the 1:1 trisradical tricationic complexes (**DB**⊂**CBPQT**)•3PF_6, (**DB**⊂**DAPQT**)•3PF_6, **MDAP**•2PF_6 and **MV**•2PF_6 (bottom).

Figure 2. (a) Variable scan-rate CV of $\mathbf{MDAP}^{2+}$ (1 mM in MeCN, 0.1 M $TBAPF_6$, 298 K) exhibiting an additional oxidation wave at +40 mV upon increasing the scan rate. (b) UV-Vis-NIR adsorption spectra (50 μM in MeCN, 298 K) of $\mathbf{DB}^{\bullet+}$, $\mathbf{DAPQT}^{2(\bullet+)}$ and $\mathbf{DB}^{\bullet+}\subset\mathbf{DAPQT}^{2(\bullet+)}$ indicating the formation of the heterogeneous 1:1 trisradical complex characterized by the appearance of an NIR band centered on 920 nm. (c) Perspective view of the crystal structure of $(\mathbf{DB}\subset\mathbf{DAPQT})^{2\bullet4+}$ showing the torsional angles and plane-to-plane separations. (d) Side-on view of the solid-state superstructure of $(\mathbf{DB}\subset\mathbf{DAPQT})^{2\bullet4+}$ demonstrating the intermolecular interactions.

Figure 3. Comparison of ^{1}H NMR spectra (500 MHz, CD_3CN, 298 K) of (a) $\mathbf{CBPQT}^{4+}$, (b) $\mathbf{AC}^{8+}$ and (c) $\mathbf{DAPQT}^{4+}$.

Figure 4. (a) EPR spectra of $\mathbf{AC}^{\bullet7+}$ and $\mathbf{SC}^{\bullet7+}$ (0.2 mM in MeCN, 298 K) displaying indiscernible hyperfine splitting patterns. (b) UV-Vis-NIR absorption spectra (50 μM in MeCN, 298 K) of $\mathbf{AC}^{\bullet7+}$ and $\mathbf{SC}^{\bullet7+}$, both showing a broad NIR absorption band centered on 1415 nm. Perspective views of X-ray crystal structures of (c) $\mathbf{AC}^{\bullet7+}$ and (d) $\mathbf{SC}^{\bullet7+}$ highlighting their torsional angles and plane-to-plane separations.

Figure 5. DPV of (a) $\mathbf{SC}^{\bullet7+}$, (b) $\mathbf{HC}^{\bullet7+}$, and (c) $\mathbf{AC}^{\bullet7+}$ (1 mM in MeCN, 0.1 M $TBAPF_6$, 200 mV s^{-1}, 298 K) showing five, six, and seven discrete redox states, respectively.

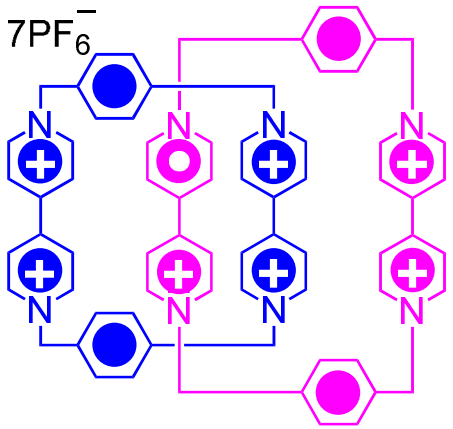

HC•7PF$_6$

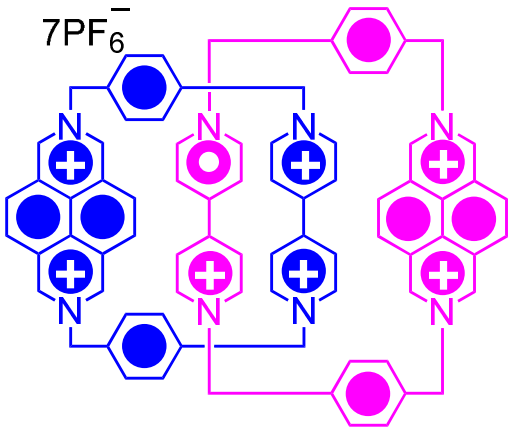

SC•7PF$_6$

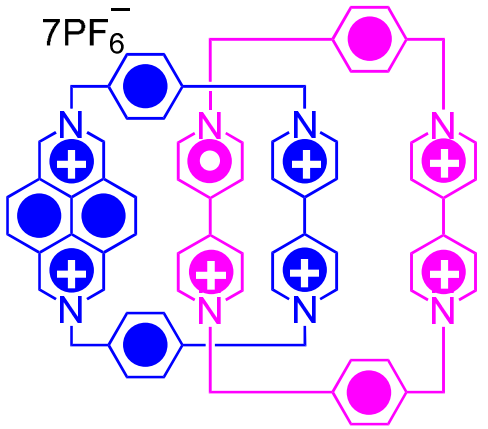

AC•7PF$_6$

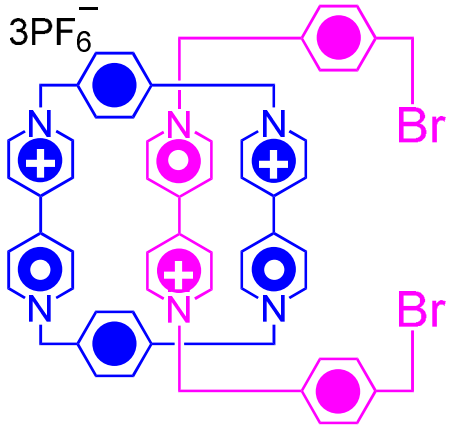

(DB⊂CBPQT)•3PF$_6$

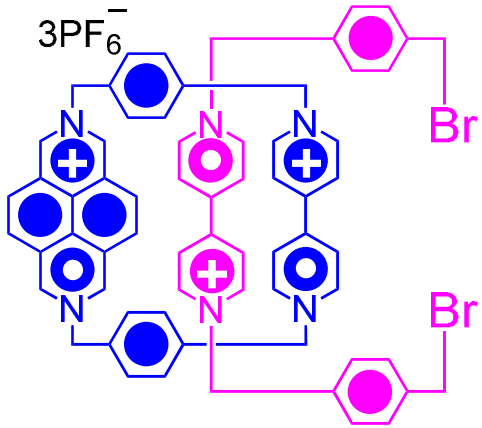

(DB⊂DAPQT)•3PF$_6$

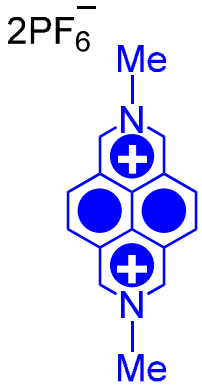

MDAP•2PF$_6$

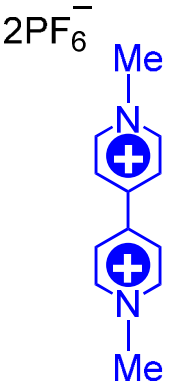

MV•2PF$_6$

Figure 1

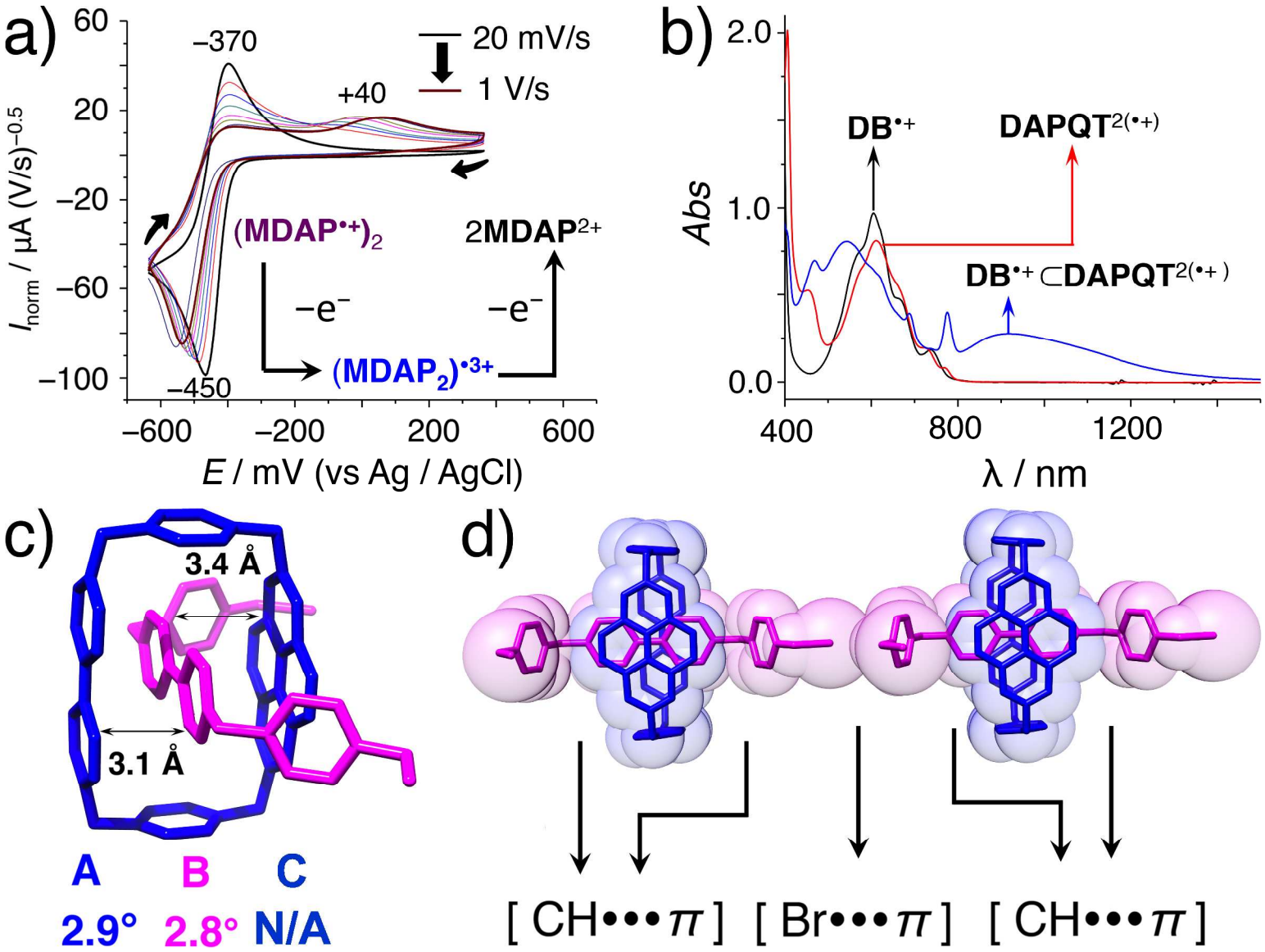
a)
60
20
−20
−60
−100
I_{norm} / μA (V/s)$^{-0.5}$
−370
+40
−450
20 mV/s
1 V/s
(MDAP•+)2
2MDAP2+
−e−
−e−
(MDAP2)•3+
−600
−200
200
600
E / mV (vs Ag / AgCl)
b)
2.0
1.0
0.0
Abs
DB•+
DAPQT2(•+)
DB•+ ⊂DAPQT2(•+)
400
800
1200
λ / nm
c)
3.4 Å
3.1 Å
A
B
C
2.9°
2.8°
N/A
d)
[CH•••π]
[Br•••π]
[CH•••π]

Figure 2

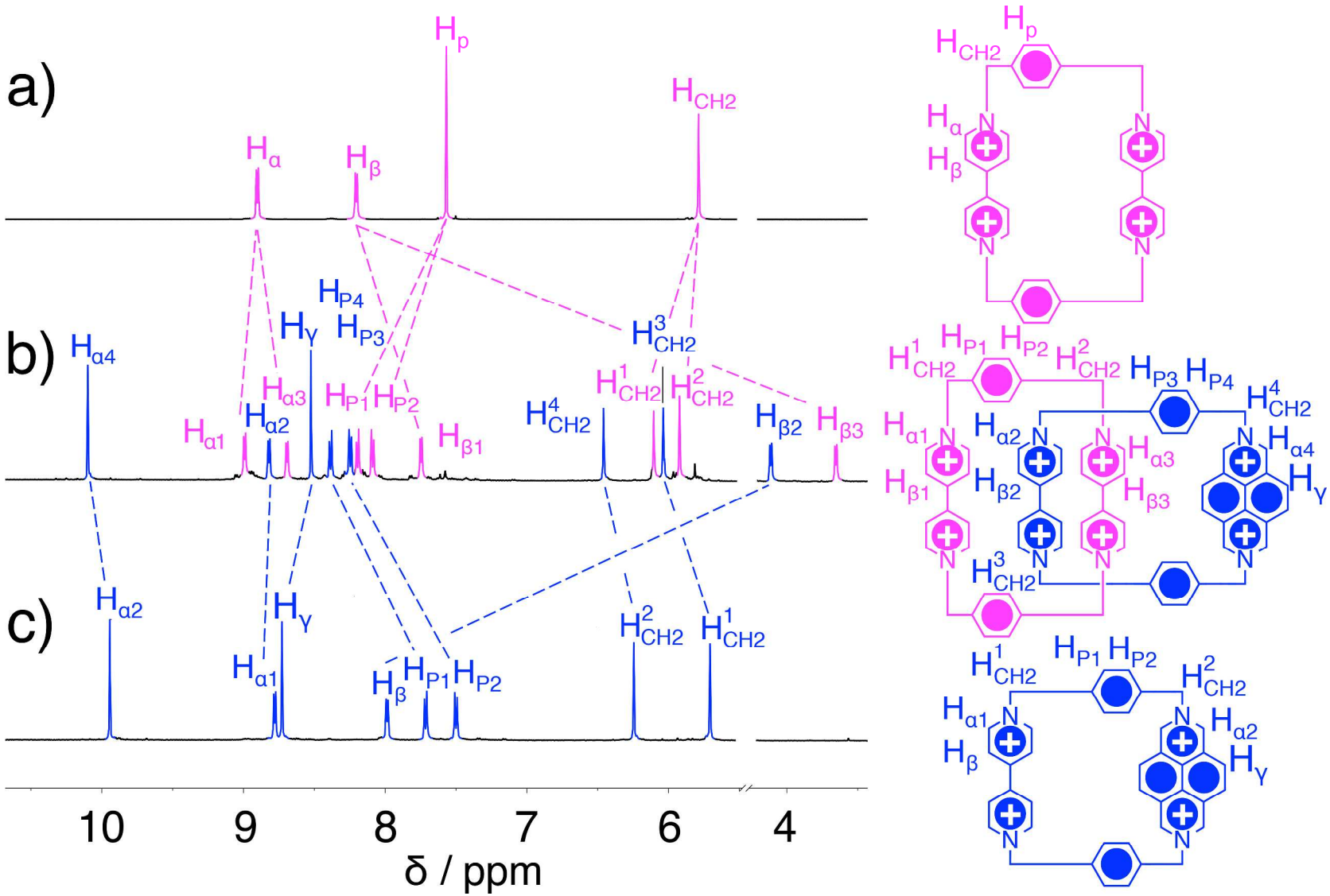
a)
b)
c)
H_p
H_{CH2}
H_α
H_β
H_{P4}
H_γ
H_{P3}
H^3_{CH2}
$H_{\alpha4}$
$H_{\alpha3}$
H_{P1}
H_{P2}
H^1_{CH2}
H^2_{CH2}
$H_{\alpha1}$
$H_{\alpha2}$
H^4_{CH2}
$H_{\beta1}$
$H_{\beta2}$
$H_{\beta3}$
10
9
8
7
6
4
δ / ppm

Figure 3

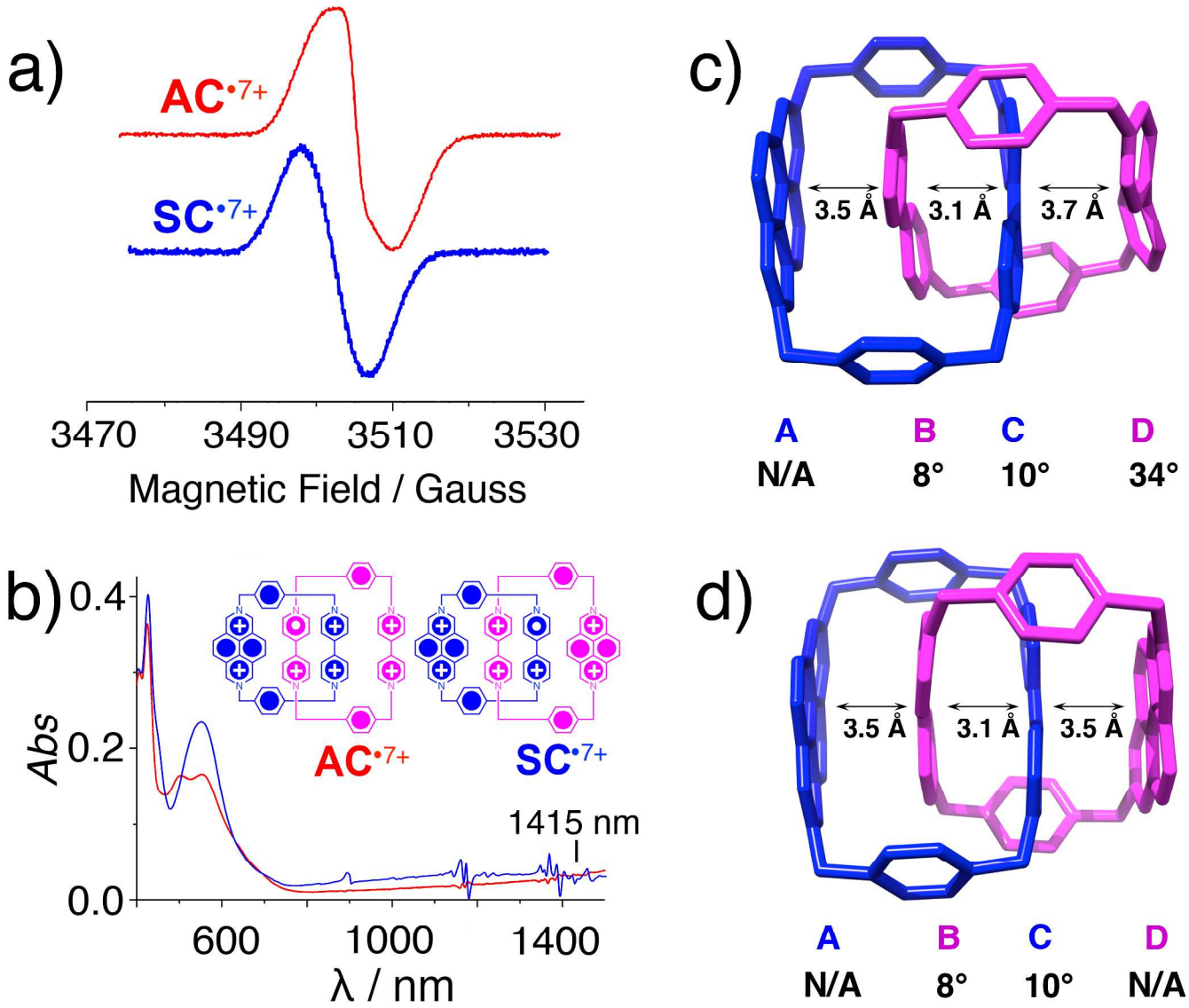
a)
AC•7+
SC•7+
3470
3490
3510
3530
Magnetic Field / Gauss
b)
0.4
0.2
0.0
Abs
AC•7+
SC•7+
1415 nm
600
1000
1400
λ / nm
c)
3.5 Å
3.1 Å
3.7 Å
A B C D
N/A 8° 10° 34°
d)
3.5 Å
3.1 Å
3.5 Å
A B C D
N/A 8° 10° N/A

Figure 4

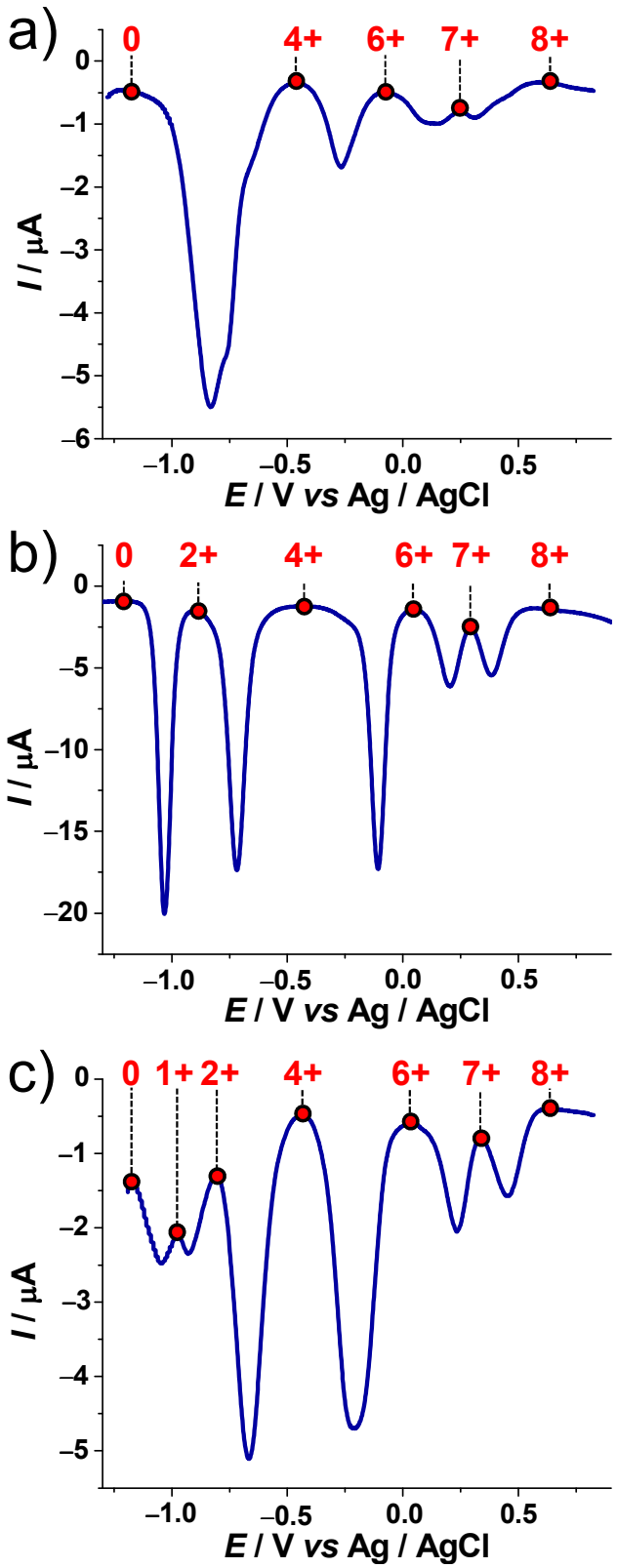
a)
0
4+
6+
7+
8+
I / μA
E / V vs Ag / AgCl
b)
0
2+
4+
6+
7+
8+
I / μA
E / V vs Ag / AgCl
c)
0
1+
2+
4+
6+
7+
8+
I / μA
E / V vs Ag / AgCl

Figure 5

TOC Graphic

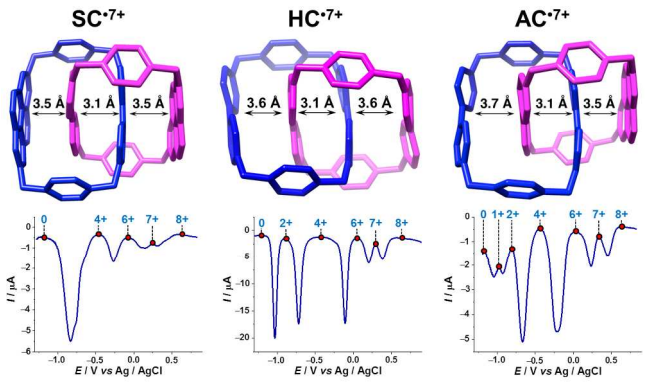
SC•7+
HC•7+
AC•7+
3.5 Å
3.1 Å
3.5 Å
3.6 Å
3.1 Å
3.6 Å
3.7 Å
3.1 Å
3.5 Å
0
4+
6+
7+
8+
0
2+
4+
6+
7+
8+
0
1+
2+
4+
6+
7+
8+
I / μA
E / V vs Ag / AgCl